Agriculture, Ecosystems and Environment 342 (2023) 108249

Contents lists available at ScienceDirect

Agriculture, Ecosystems and Environment

journal homepage: www.elsevier.com/locate/agee

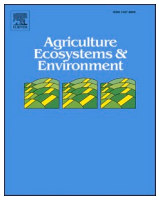

Long-term N addition accelerated organic carbon mineralization in aggregates by shifting microbial community composition

Yu Zhang [a,b,c], Zhouping Shangguan [a,b,c,*]

[a] The Research Center of Soil and Water Conservation and Ecological Environment, Chinese Academy of Sciences and Ministry of Education, Yangling, Shaanxi 712100, China
[b] Institute of Soil and Water Conservation, Chinese Academy of Sciences and Ministry of Water Resources, Yangling, Shaanxi 712100, China
[c] University of Chinese Academy of Sciences, Beijing 100049, China

ARTICLE INFO

Keywords:
SOC mineralization
Microbial community composition
Soil aggregates
Co-occurrence network
N addition

ABSTRACT

Nitrogen application in agroecosystem maintains and improves soil fertility while affecting organic carbon mineralization (C_{min}). Soil aggregates play a crucial role in soil organic carbon (SOC) turnover. However, the cumulative C_{min} and underlying microbial mechanisms responses to long-term N addition at aggregate scales remain unclear. Hence, a 16-year field N addition field experiment was conducted on winter wheat (*Triticum aestivum* L.) at three N levels: 0 (N0), 180 (N180), and 360 (N360) N ha^{-1}. Overall, long-term N addition significantly altered the C_{min}, bacterial and fungal community composition and bacterial and fungal co-occurrence patterns in four aggregate fractions (large macroaggregates, small macroaggregates, micro-aggregates, and silt-clay fractions). Specifically, N addition facilitated a more copiotrophic microbial community, with a significant increase in the relative abundances of *Proteobacteria*, *Gemmatimonadota*, and *Ascomycota*, and a significant decrease in the relative abundances of *Actinomycetales*, *Acidimicrobiales*, and *Basidiomycota*. The addition of N led to more complex and tight microbial networks with more nodes, higher average degrees, shorter average path lengths, and greater connectivity. These microbial changes accelerated C_{min} in aggregates; however, the main microbial mechanisms varied with aggregate size and C_{min} in silt-clay fractions was mainly influenced by microbial community composition. These results indicate that the spatial heterogeneity of resources available in different aggregate sizes is strongly selected for microbial life strategies and influences the distribution of microbial communities, thereby affecting the C_{min} processes. Overall, our study provides a fundamental understanding of the microbial regulation of SOC turnover at an aggregate scale and highlights the importance of network topological patterns.

1. Introduction

Agroecosystems rely on N application to maintain and improve soil fertility, and the soil organic carbon (SOC) turnover determines soil fertility and sustainability (Wang et al., 2021). Soil microorganisms comprise a vital part of ecosystems, regulate nutrient conversion and SOC turnover, and are highly sensitive to environmental change (Moorhead et al., 2013). N addition can affect C turnover by changing soil properties (e.g., soil N availability, base cations composition, pH, etc.), which directly impacts soil microorganisms (e.g., biomass, extracellular enzymes, and community structure) (Wang et al., 2022). Additionally, N addition significantly increases crop yield, along with affecting plant physiology and ecology, which in turn indirectly affects microbial activity and SOC turnover (Fan et al., 2021b). Hence, it is necessary to fully understand how microbes governing SOC turnover respond to N addition.

Soil aggregates constitute the structure of soil components, providing heterogeneous microhabitats for microorganisms and physically protected SOC sequestration, which are crucial for SOC turnover (Six et al., 2004). The amount and complexity of SOC may be unevenly distributed within the aggregate fractions and exhibit different activities toward microorganisms, resulting in different SOC turnover rates (Six et al., 2000). In general, macroaggregates contain more fresh, labile, and easily decomposed plant-derived SOC (Wang et al., 2015), whereas the SOC in smaller aggregates is mostly characterized by high aromaticity, longer turnover time, and difficulty in decomposing microorganisms

* Correspondence to: Institute of Soil and Water Conservation, Xinong Rd. 26, Yangling, Shaanxi 712100, China.
E-mail address: shangguan@ms.iswc.ac.cn (Z. Shangguan).

https://doi.org/10.1016/j.agee.2022.108249
Received 15 July 2022; Received in revised form 15 October 2022; Accepted 25 October 2022
Available online 31 October 2022

(Jia et al., 2019). Moreover, the pore characteristics of the aggregates varied with the aggregate sizes. Compared with microaggregates, macroaggregates have larger soil pores, increasing material and oxygen transport, facilitating microbial activities, and promoting SOC mineralization (C_{min}) and CO_2 release (Ruamps et al., 2011). Whereby, SOC turnover in microaggregates is more likely to reach a steady-state (Tian et al., 2016). Nevertheless, inconsistent results of C_{min} within aggregate fractions have also observed that equivalent among aggregates (Rabbi et al., 2014) or microaggregates hold larger C_{min} (Wang et al., 2021). Therefore, further studies on C_{min} at the aggregate scale are needed to in-depth understand the response of SOC turnover to N addition.

Previous studies have shown that the responses of microbial community composition and function to N addition lack consensus in different ecosystems or in the same ecosystem with different N addition levels (Jia et al., 2020). Wang et al. (2022) found that N addition altered bacterial and fungal diversity and community structure, whereas the effects were different. Inconspicuous differences in the effects of N enrichment on sub-surface soil microbial community structure have emerged in temperate steppe ecosystem (Zeng et al., 2016). Furthermore, prior N addition studies focused more on bulk soils, neglecting the response of microbial communities in different aggregate fractions. Microbial communities may respond uniquely to various nutrients, water, and oxygen microhabitats in aggregates (Fox et al., 2018). Microorganisms may be distributed in distinct niches based on their substrate preferences and nutrient acquisition strategies (Banerjee et al., 2016). Macroaggregate C turnover may be dominated by *R*-strategists (copiotrophs, in response to fresh C), whereas that in microaggregates may be dominated by *K*-strategists (oligotrophs, in response to recalcitrant C) (Fan et al., 2021a). To some extent, microaggregates hold larger specific surface areas and relatively stable water availability lead to increased microbial adhesion (Rabbi et al., 2016; Bach et al., 2018). Additionally, microorganisms co-occurrence through direct or indirect interactions (mutualism, competition, parasitism, predation, etc.), forming a complex symbiotic network in the soil (Barberán et al., 2012). Co-occurrence networks can effectively reveal microbial interactions and how they interact with environmental parameters (Deng et al., 2012). Identifying microbial interactions may be crucial for disentangling the underlying mechanism of SOC turnover. Notwithstanding, little is known about the alterations of microbial interactions at the aggregate scale under N addition and how to modulate C_{min}.

In current work, we established a long-term (16-year) N addition field experiment to assess the influence of N addition on C_{min} in four aggregate fractions (large macroaggregates, small macroaggregates, microaggregates, and silt-clay fractions). We also analyzed the microbial community composition and interactions using high-throughput sequencing technology in aggregate fractions. This study addressed the following questions. i) Does the C_{min} vary in different aggregate fractions in response to long-term N addition? ii) Do microbial communities and their co-occurrence networks vary in different aggregate fractions induced by N addition? iii) How do microorganisms mediate C_{min} in different aggregate fractions under nitrogen addition?

2. Materials and methods

2.1. Site description and experimental design

The study site is located at the Institute of Soil and Water Conservation, Chinese Academy of Sciences (34°17′56″N, 108°04′7″E, Yangling, Shaanxi Province), in the southern part of the Loess Plateau. The area belongs to the warm temperate zone semi-humid continental monsoon climate, with an average annual precipitation of 632 mm and a mean annual temperature of 13 °C. The soil is classified as Eum-Orthic Anthrosol in the Chinese Soil Taxonomy and as *Udic Haplustalf* in the US Department of Agriculture. The initial soil physicochemical properties were listed in Table S1 (Zhong et al., 2015).

The long-term experiment was established in 2004 using a completely randomized trial design with three N application levels: 0 kg N ha^{-1}, 180 kg N ha^{-1}, and 360 kg N ha^{-1} of urea (hereafter referred to as N0, N180 and N360, respectively). The bare field (BL) was the control area, and three 2 m × 3 m replicate plots were used for each treatment. Winter wheat (Changhan No. 58) was sown in early October every year and harvested at the end of the following May, and a winter wheat-summer fallow cropping pattern was adopted. No irrigation and regular weeding were performed during the study period.

2.2. Field sampling and aggregate fractionation

In May 2020, five undisturbed soil samples were randomly obtained from a depth of 0–20 cm in each plot for aggregate fractionation. To minimize microbial community destruction during sieving and the effects of dissolved organic carbon in the aggregates, the optimal moist sieving method was adopted to isolate the aggregates (Dorodnikov et al., 2009). Briefly, fresh undisturbed soil was gently parted along natural breakpoints and sieved to 8 mm. Then, 100 g of soil was transferred to a sleeve sieve, and four aggregate fractions were separated: > 2 mm (large macroaggregates), 0.25–2 mm (small macroaggregates), 0.053–0.25 mm (microaggregates), and < 0.053 mm (silt-clay fraction), respectively. This process was repeated to ensure that all parameters were measured. Then, a fresh subsample portion was used for DNA extraction. Another fresh soil portion was stored at 4 °C (within 3 days) to measure dissolved organic carbon (DOC), dissolved organic nitrogen (DON), and extracellular enzyme activities. The remaining sub-sample portion was air-dried to determine soil physicochemical properties. Soil pH was measured using a glass electrode meter at a soil and water ratio of 2.5:1. The SOC was estimated using the H_2SO_4-$K_2Cr_2O_7$ method (Nelson and Sommers, 1982). Total soil N was analyzed using the Kjeldahl method (Bremner and Mulvaney, 1996). DOC and DON were extracted with 0.5 M K_2SO_4 and measured by a Shimadzu TOC-TN analyzer (Shimadzu Corp., Kyoto, Japan) (Badr et al., 2003). Soil total P (STP) was detestation by H_2SO_4–$HClO_4$ and determined by molybdenum antimony blue colorimetry-(Murphy and Riley, 1962), and available P (SAP) was extracted with 0.5 M $NaHCO_3$ (Olsen and Sommers, 1982). Soil ammonium-nitrogen (NH_4^+) and nitrate-nitrogen (NO_3^-) were extracted with 2 M KCl and analyzed using a continuous-flow auto-analyzer (Autoanalyser, Bran + Luebbe, Germany).

2.3. Potential C mineralization

Potential C mineralization was determined via a microcosm incubation experiment. Fresh aggregate fractions (30 g) were placed in 250 mL glass jars and adjusted to a 60% field holding capacity with distilled water pre-incubated at 25 ℃ for 7 days. The aggregate fraction sample of each treatment was repeated three times, and three empty jars without samples were used for reference readings. Water content was monitored during incubation. After pre-culture, headspace samples were collected with a 30 mL syringe at 1, 3, 5, 7, 10, 14, 21, 28, and 35 d of incubation to determine the amount of CO_2, using gas chromatography (AgilentC6890). The jars were opened for 1 h after sampling to maintain the oxygen level. The potential Cmin was quantified as the amount of C produced per unit of soil (mg CO_2-C kg^{-1} soil), and the cumulative C_{min} was calculated according to Zhang et al. (2021b).

2.4. Enzymatic analyses

Four hydrolases: *β*-1,4-glucosidase (BG), *β*-D-cellobiohydrolase (CBH), leucine aminopeptidase (LAP), and N-acetyl-*β*-D-glucosaminidase (NAG) were quantified using a slightly modified fluorometric measurement protocol with fluorescent compounds 4-methylumbelliferone (MUB) and 7-amino-4-methylcoumarin (AMC) according to Bell et al. (2013). Briefly, 1 g of soil was mixed with 50 mL of 50 mM Tris-HCl buffer (the pH was the same as the soil pH) using a magnetic stir plate. Subsequently, 150 μL of the soil slurry and 50 μL of the substrate

solution were pipetted into the wells of a 96-well flat-black-bottomed microplate. The microplates were incubated for 2 h (BG, LAP), and 4 h (CBH, NAG) at 25 °C in the dark, and the reactions were stopped by adding 50 μL of 1 M NaOH. Standard curves were plotted for the MUB and AMC for each soil sample. All fluorescence values were quantified using a microplate fluorometer (Synergy, BioTek, USA) at 365 nm excitation and 460 nm emission. The soil extracellular enzyme activity was recorded as nmol activity g^{-1} soil h^{-1}.

2.5. DNA extraction and network analysis

Total genomic DNA from aggregate fractions (0.5 g) was extracted using the MP FastDNA Spin Kit for soil (MP Biomedicals, Solon, OH, USA), following the manufacturer's instructions. DNA concentration and purity were quantified using a NanoDrop2000 (Thermo Scientific, Waltham, USA). Illumina MiSeq sequencing was used to investigate the soil fungal and bacterial community composition. Bacterial 16 S rRNA genes were PCR-amplified using primers 338 F (5′-ACTCCTACGGGAG GCAGCAG-3′) and 806 R (5′-GGACTACHVGGGTWTCTAAT-3′). Fungal ITS was amplified using ITS1F (5′-CTTGGTCATTTAGAGGAAGTAA-3′) and ITS2R (5′-GC TGCGTTCTTCATCGATGC-3′). The PCR reaction conditions were as follows: denaturation at 95 °C for 3 min, followed by 30 cycles of 95 °C for 30 s, 55 °C for 30 s, and 72 °C for 45 s, and finally, being held at 72 °C for 10 min. The purified PCR product was sequenced on an Illumina MiSeq PE300 platform. QIIME was used for quality control and original data filtering, and 97% of the similar sequences were clustered into OUT using UPARSE software. The pair-end reads were spliced using Flash (v1.2.11), and the raw sequences were quality-filtered using QIIME (v1.9.1) and clustered using UPARSE (v7.0.1090) at a 97% similarity threshold. FungalTraits v0.03 database was used to classify potential functional groups of fungi (Polme et al., 2020).

Bacterial and fungal co-occurrence networks were constructed using the Molecular Ecological Network Analysis Pipeline (Deng et al., 2012). The minimum occurrence of quality-filtered and clustered OTUs was set to half of the sample size, and Spearman's correlation was performed to calculate the correlation between pairwise OTUs. Based on random matrix theory (RMT), the network properties, individual node centrality, and co-occurrence network modularity were calculated. The keystone species were OTUs with a high degree, eigenvector centrality, and betweenness. Co-occurrence networks were visualized using Geophi0.9.2.

2.6. Statistical analyses

One-way ANOVA and Duncan's test were performed to determine the impacts of N addition on soil parameters and cumulative C_{min} ($p < 0.05$). Two-way ANOVA was applied to examine the effects of N addition, soil aggregate sizes, and their interactions on all response variables using SPSS Statistics 22.0 (IBM). Permutation multivariate analysis of variance (PERMANOVA) and principal coordinates analysis (PCoA) sequenced at the OUT level based on Bray-Curties distance were used to investigate the microbial community composition effect on N addition and aggregate fractions. The "labdsv" package was used to analyze the OTU level data. The PERMANOVA was tested using Adonis from the "vegan" package in R (v 3.2.1).

The Mantel test was used to analyze the correlation between soil properties and microbial co-occurrence networks, and random forest modeling was used to explore the relative importance of predictors affecting cumulative C_{min}. The PLS-PM model was used to investigate the direct and indirect interactions between soil properties (soil chemical properties), microbial community composition (bacterial and fungal communities), network properties (average degree, average path length, clustering coefficient, and other topological features), and C_{min}. We further evaluated the microbial mechanisms of C_{min} in aggregates in response to N addition. The model fit was assessed based on the goodness of fit (GOF). The "randomForest" package, "vegan" package, and "PLS-PM" package were used for the analyses. Graphs were plotted using Origin 2021.

3. Results

3.1. Changes in soil physicochemical properties and C_{min}

The variations in soil physicochemical properties were shown in Table 1. Compared with N0, pH decreased significantly, TN increased significantly under N addition ($P < 0.05$; Table 1), and SOC increased but showed no significant difference. In addition, the proportions of microaggregates in BL were significantly higher than those in the N-treated plots ($P < 0.05$). And the proportion of large macroaggregates increased in the N180 plots, and that of the silt-clay fraction decreased, whereas the difference was insignificant in comparison with other N treatments. The N360 plots exhibited a similar trend, and the silt–clay fraction proportion decreased significantly ($P < 0.05$). The SOC content distribution in the large macroaggregates significantly increased in the N180 treatment ($P < 0.05$; Fig. 1a). The SOC concentration within aggregates differed significantly ($P < 0.001$), and all exhibited the order of microaggregates > macroaggregates > silt-clay fractions (Fig. 1b). N180 significantly increased the SOC concentration in large and small macroaggregates ($P < 0.05$), whereas no significant differences were observed in other aggregate fractions. The increase in SOC concentration in macroaggregates was greater than that in small aggregate sizes. Similar to the SOC concentration, the cumulative C_{min} was significantly increased by N addition within aggregate fractions ($P < 0.001$; Fig. 1c) and was the highest in microaggregates and the lowest in silt-clay fraction. Among different N treatments, the cumulative C_{min} in N180 was greater than that in N360, and the increase in N360 was the largest in the small macroaggregates among the aggregate fractions.

3.2. Changes in enzyme activity

The total enzyme activity was significantly affected by N addition ($F = 543.2$, $P < 0.001$) and aggregate fractions ($F = 417.9$, $P < 0.001$) (Fig. 2). The total enzyme activities were higher at N180 and N360 than at N0 ($P < 0.05$), and the individual enzymes displayed a similar pattern. Meanwhile, the highest activities were all obtained in microaggregates, and the distribution of extracellular enzyme activities followed the order: microaggregates > small macroaggregates > large macroaggregates > silt-clay fractions. Compared with N0, the increase in total enzyme activity was greatest in microaggregates; N180 and N360 increased by 37.5 % and 20.3 %, respectively, whereas the increase in large macroaggregates was the smallest. Regarding individual enzyme activity, the increase induced by N addition was the smallest in large macroaggregates and the largest in small macroaggregate.

3.3. Changes in microbial community composition

In summary, *Actinobacteriota*, *Proteobacteria*, *Acidobacteriota*, *Chloroflexi*, and *Gemmatimonadota* were the main phyla in the bacterial community. N addition significantly decreased the relative abundance of *Actinobacteriota* and *Acidobacteriota*, and had a significant increase of *Proteobacteria* and *Gemmatimonadota* ($P < 0.05$). Bacterial distribution within the aggregate fractions was inhomogeneous. The relative abundance of *Actinobacteriota* and *Proteobacteria* significantly increased with decreasing aggregate size, whereas the relative abundance of other phyla exhibited the opposite trend ($P < 0.05$; Fig. 3). Both *Actinobacteriota* and *Gemmatimonadota* showed the greatest variation in large macroaggregates. As for fungi, *Ascomycota*, *Basidiomycota*, and *Mortierellomycota* were the dominant phyla. The relative abundance of *Ascomycota* significantly increased with N addition, while that of *Glomeromycota* and *Basidiomycota* decreased, and the *Basidiomycota* only significantly decreased under N360 treatment in microaggregates ($P < 0.05$). The relative abundance of *Ascomycota* and *Mortierellomycota*

Table 1
Soil physicochemical properties under long-term N addition.

	pH (H_2O) 1:2.5	SOC (g kg^{-1})	TN (g kg^{-1})	TP (g kg^{-1})	C/N	DOC (mg kg^{-1})	> 2 mm (%)	0.25–2 mm (%)	0.053–0.25 mm (%)	< 0.053 mm (%)
BL	8.4 ± 0.0a	8.8 ± 1.4b	1.1 ± 0.0c	0.9 ± 0.25a	7.3 ± 0.6b	143 ± 8b	32.6 ± 1.9b	54.6 ± 1.4a	7.3 ± 0.3a	2.1 ± 0.2a
N0	8.3 ± 0.0b	9.8 ± 0.1a	1.2 ± 0.1b	0.9 ± 0.1a	8.5 ± 0.3a	209 ± 13a	33.3 ± 0.8ab	53.2 ± 0.7a	6.1 ± 0.2b	1.5 ± 0.2a
N180	8.3 ± 0.00c	10.3 ± 0.1a	1.2 ± 0.1a	0.9 ± 0.3a	8.2 ± 0.3a	236 ± 7a	36.2 ± 0.6a	52.6 ± 0.7a	6.0 ± 0.3b	1.4 ± 0.2ab
N360	8.2 ± 0.0d	10.1 ± 0.0a	1.2 ± 0.1ab	0.9 ± 0.0a	8.3 ± 0.4a	226 ± 3a	34.0 ± 0.9ab	55.1 ± 1.4a	6.2 ± 0.3b	1.4 ± 0.2b

Note: Values are the means ± standard deviation of three plots, BL, bare land; N0, 0 kg N ha^{-1}; N180: 180 kg N ha^{-1}; N360: 360 kg N ha^{-1}; SOC: soil organic carbon; TN: soil total nitrogen; TP: soil total phosphorous; C/N: soil organic carbon to soil total nitrogen ratio; DOC: soil dissolved organic carbon. Different letters indicate significant differences at $P < 0.05$ in different treatments.

were greater in small aggregate sizes, whereas *Basidiomycota* and *Glomeromycota* was more abundance in large macroaggregates. The PCoA showed that the bacterial and fungal communities were separated in aggregate fractions under N addition, and PERMANOVA further showed that long-term N addition and aggregate fractions significantly changed the structure of the bacterial and fungal communities (bacteria: N, R^2 =0.328, $P < 0.001$; aggregate fractions, R^2 =0.195, $P < 0.001$; fungi: N, R^2 =0.269, $P < 0.001$; aggregate fractions, R^2 =0.318, $P < 0.001$) (Fig. 4, Table S2).

3.4. Co-occurrence network

Bacterial and fungal co-occurrence networks were constructed based on Spearman's correlation to determine the impacts of N addition on microbial interactions (Fig. 5). All constructed networks conformed to a power-law distribution (R^2 variation range 0.88–0.94, $P < 0.001$), exhibiting scale-free and non-random topological features. Compared with treatment without N (BL and N0), both bacterial and fungal co-occurrence networks had a higher number of nodes and edges, and a higher average degree under N addition (N180 and N360) (Table 2), which reflected the more complex microbial co-occurrence networks with N addition. N addition enhanced connectivity and shortened the average path length (Table 2), thereby tightening the network. Additionally, the positive correlations between the bacterial and fungal nodes were greater than the negative correlations across all treatments, but N addition reduced the ratio of positive to negative correlations (Table 2). The keystone taxa without N addition were *Actinobacteria* and *Proteobacteria* of bacteria and *Ascomycota* and *Basidiomycota* of fungi, whereas keystone taxa with N addition were *Actinobacteria* and *Ascomycota*, respectively. Further analysis of the co-occurrence network with different N addition treatments in aggregate fractions (Table S3 and S4) revealed that N addition resulted in a significant increase in the number of fungal and bacterial nodes, average degree, and eigenvector centralization, and a significant decrease in the average path length, centralization betweenness, and centralization closeness ($P < 0.05$). As the aggregate size decreased, the average degree, eigenvector centralization significantly increased, and the average path length, global clustering coefficient significantly decreased ($P < 0.05$). Meanwhile, the modularity was maximum in large macroaggregates, and the number of nodes and average degree were the largest in microaggregates. The mantel test showed that the co-occurrence network parameters were significantly correlated with the environmental factors (R=0.644, $P < 0.001$).

3.5. Relationships among soil properties, microbial traits and C_{min}

Random forest analysis showed the relative importance of the predictors affecting the cumulative C_{min} (Table S5). The PLS-PM model was performed using the main predictors to disentangle the direct and indirect interactions among soil properties (soil chemical properties), microbial community composition (represented by the first principal components of PCoA), network properties (nodes, average degree, path length, clustering coefficient, and other topological features), enzyme activity (BG, CBH, LAP, and NAG), and C_{min} in aggregates (Fig. 6). Except for large macroaggregates, the soil properties had an insignificant effect on enzyme activity. Specifically, the bacterial network properties and fungal community composition significantly promoted enzyme activity in large and small macroaggregates, explaining 95.5 % of the variation in enzyme activity within small macroaggregates (Fig. 6a, b). Bacterial community composition and fungal network properties jointly influenced the enzyme activity in the microaggregates (Fig. 6c). As for the silt-clay fractions, enzyme activity was affected mainly by the bacterial and fungal community composition and consequently improved cumulative C_{min} (Fig. 6d).

4. Discussion

4.1. Effects of N addition on microbial community composition within aggregates

Soil microorganisms comprise a vital part of ecosystems, and participate in nutrient transformation and SOC turnover (Moorhead et al., 2013). In this study, long-term N addition significantly altered soil microbial community composition (Fig. 3). Specifically, N addition significantly reduced the relative abundance of *Actinobacteria* and *Acidobacteria*, while significantly increasing the relative abundance of *Proteobacteria* and *Gemmatimonadota* ($P < 0.05$). Actinomyces are generally considered to possess competitive advantages under stress conditions, participate in the decomposition of soil humus and other resistant SOM, and make profound contributions to lignocellulosic degradation genes (Ren et al., 2020). Thus, variation in their abundance may be coupled with recalcitrant C turnover (Zhang et al., 2021a). Most *Acidobacteria* are also associated with low carbon turnover and have been identified as oligotrophic microorganisms (Zeng et al., 2016). In contrast, *Proteobacteria* are more likely to be R-strategist copiotrophs (with relatively rapid growth rates) that severely depend on nutrient availability and sensitivity to environmental changes (Fierer et al., 2012). Previous studies have also shown that N addition leads to a shift in bacterial communities toward copiotrophs (Ling et al., 2017). Simultaneously, N addition significantly increased the relative abundance of *Ascomycota*, which dominate the fungal community, including those that produce extracellular enzymes and cleavage lignin and cellulose (Su et al., 2020), while the relative abundance of *Basidiomycota* decreased. The main reason for this may be that *Ascomycota* are more tolerant to high N environments than *Basidiomycota* (Allison et al., 2010). N addition enhanced the microbial C source, promoted saprophytes growth, and boosted their competitiveness, leading to a decline in the mostly non-saprotrophic *Basidiomycota* (He et al., 2021). Notably, several *Ascomycetes* species have been assigned as plant pathogens (Lombard et al., 2015). We predicted fungal function based on fungal

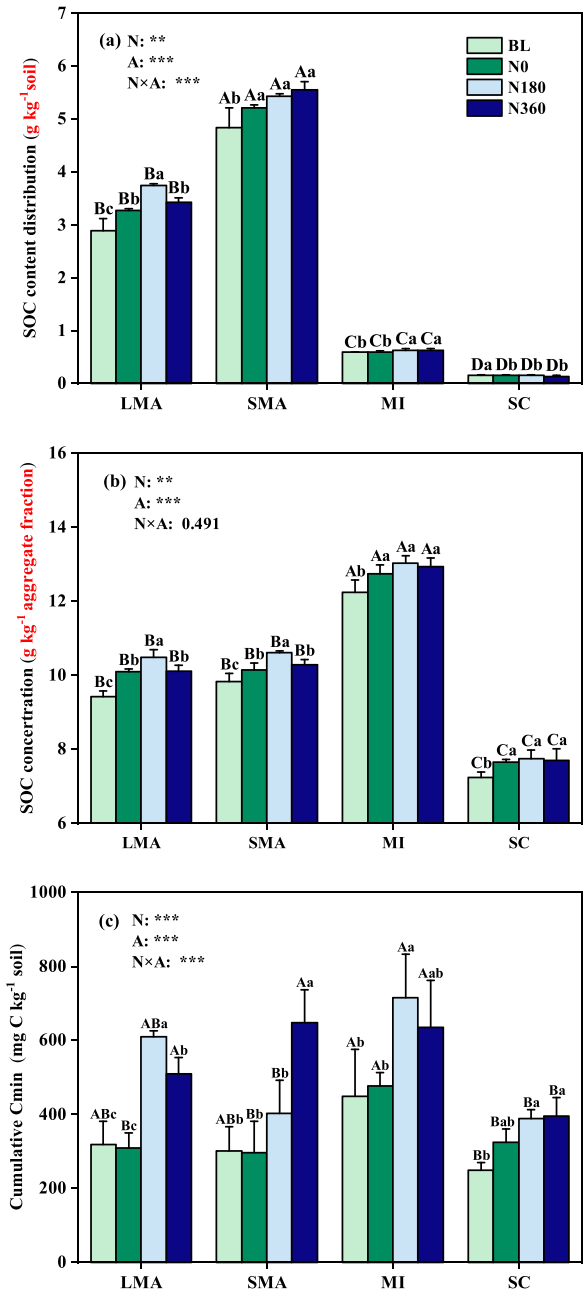

Fig. 1. Effects of the N addition and aggregate fractions on the SOC content distribution (A), SOC concentration (B), and cumulative C mineralization (C). LMA, large macroaggregate; SMA, small macroaggregate; MI, microaggregate; SC, silt-clay fractions. Error bars represent the standard deviation of the means (n = 3). Different capital letters indicate significant differences among different aggregates within the same treatment ($P < 0.05$). Different small letters indicate significant differences among treatments for the same aggregate fraction at ($P < 0.05$). Asterisk shown for N, A, and N × A represent the p values, *** $P < 0.001$, ** $P < 0.01$, * $P < 0.05$, generated from two-way ANOVA tests for the effects of nitrogen addition, aggregate fractions, and interaction between the two, respectively.

traits and found that N addition increased plant pathogens and soil saprotrophs (Table S6). However, this simple estimation of function is only at the taxonomic level, and further validation is needed. Meanwhile, slow-growing oligotrophic fungi *Basidiomycota* may be more capable of degrading recalcitrant SOM than *Ascomycetes* (Wang et al., 2019). N addition induced an increase in DOC in this study, which may also have led to an increase in *Ascomycetes*. Furthermore, *Glomeromycota* decreased with increasing N, mainly because N input enhanced the available nutrients for plants (Table S7), disconnecting the dependence of host plants on nutrient uptake from arbuscular mycorrhizal fungi (AMF). Based on the above information, in combination with the results of the correlation analysis (Table S8), it was further demonstrated that N addition strongly selects for microbial lifestyles.

Additionally, aggregate fractions significantly affected the microbial community composition in this study. The distribution of microorganisms in the aggregate fractions was inhomogeneous. As for bacteria, the relative abundance of *Actinobacteriota* significantly increased with decreasing particle size, while the relative abundance of *Acidobacteria* and *Gemmatimonadota*, *Chloroflexi* exhibited the opposite trend ($P < 0.05$; Fig. 3). In general, macroaggregates contain more labile plant-derived SOC, while SOC in smaller aggregate sizes is mostly high in aromaticity and is difficult to decompose (Jia et al., 2019). Consequently, *Actinobacteriota* showed higher abundance in the microaggregates, which is in accordance with the results of Su et al. (2020). Correlation analysis showed that *Proteobacteria* was highly significantly positively correlated with DOC (Table S8) and microaggregates had the highest SOC concentrations, resulting in *Proteobacteria* being the highest in microaggregates. In contrast, *Acidobacteria* were responsible for soil aggregate stability and were more conducive to distributing in macroaggregates (Zheng et al., 2018). Compared to bacteria, the effect of aggregate fractions on fungi was greater than that of N addition (Fig. 4, Table S2). This indicates the complex impacts of N addition on soil microorganisms and demonstrates the different sensitivities of microorganisms to environmental changes (Wang et al., 2022). The relative abundance of *Ascomycota* and *Mortierellomycota* were greater in small aggregate sizes, whereas *Basidiomycota* and *Glomeromycota* were more abundant in large macroaggregates. The effects of N on *Ascomycota* and *Basidiomycota* were the largest in large macroaggregates. This was mainly due to the heterogeneous distribution of available resources, porosity, and water within different aggregate sizes, which affected the microbial community composition (Rabbi et al., 2016; Bach et al., 2018). Therefore, microaggregates had higher nutrient content, larger specific surface area, and more stable water availability compared to macroaggregates, which may have been more favorable for microbial adhesion (Six et al., 2002; Ruamps et al., 2011; Bimueller et al., 2016; Rabbi et al., 2016), and in turn led to a relatively higher abundance of copiotroph *Ascomycota* (Zhao et al., 2021). Moreover, *Ascomycota* and *Mortierellomycota* are mostly saprophytic fungi, and the SOC structure of microaggregates is more complex, which may also lead to more abundant microorganisms (Su et al., 2020). Nevertheless, Basidiomycota have relatively weak competitiveness and prefers to inhabit large macroaggregates with high porosity and low environmental pressure (Li et al., 2020). Our unpublished results indicated that AMF was related to aggregate stability, promoted the aggregation of large aggregates, and was fixed on macroaggregates. In other words, the spatial nutrient availability heterogeneity at different aggregate fraction sizes strongly selected microbial lifestyles and influenced the distribution of microbial communities. Collectively, N addition and aggregate size affected the microbial community structure.

4.2. *Effects of N addition on microbial interactions within aggregates*

Microorganisms coexist in the environment through direct or indirect interactions (including mutualism, competition, parasitism, predation, etc.), and studies have shown that this coexistence can have a significant effect on carbon turnover by altering energy and material flow pathways or by changing species abundance (Banerjee et al., 2016). Microbial co-occurrence networks visualize microbial interactions (Barberán et al., 2012). In this study, the bacterial and fungi co-occurrence networks were mainly positively correlated (Table 2), indicating the cooperative behavior among these microorganisms (Berry and Widder, 2014). N addition significantly changed the topological parameters of the bacterial and fungal co-occurring networks

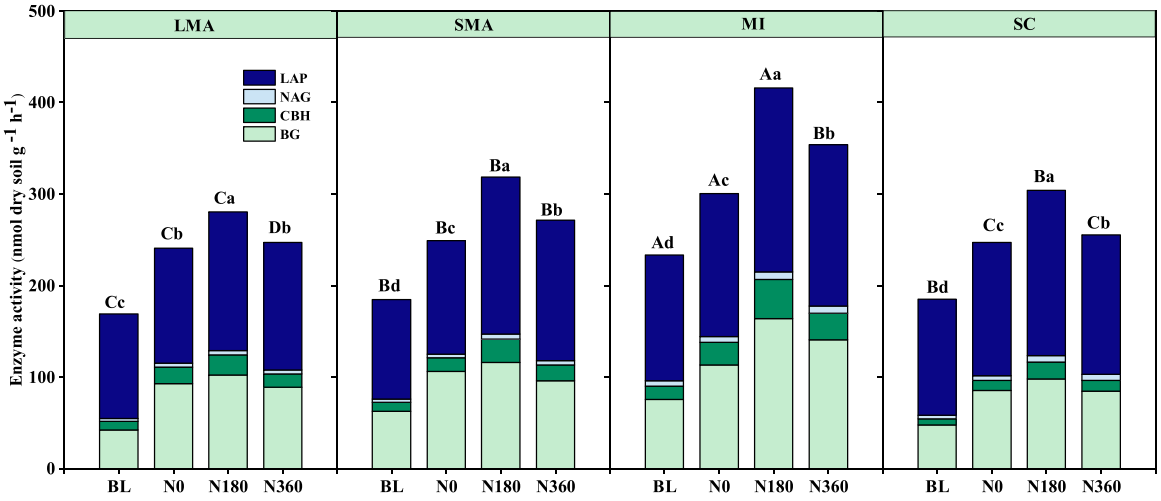

Fig. 2. Effect of the N addition on the enzyme activity in the aggregate size fractions. LMA, large macroaggregate; SMA, small macroaggregate; MI, microaggregate; SC, silt-clay fractions. Different capital letters indicate significant differences among different aggregates within the same treatment ($P < 0.05$). Different small letters indicate significant differences among treatments for the same aggregate fraction at ($P < 0.05$).

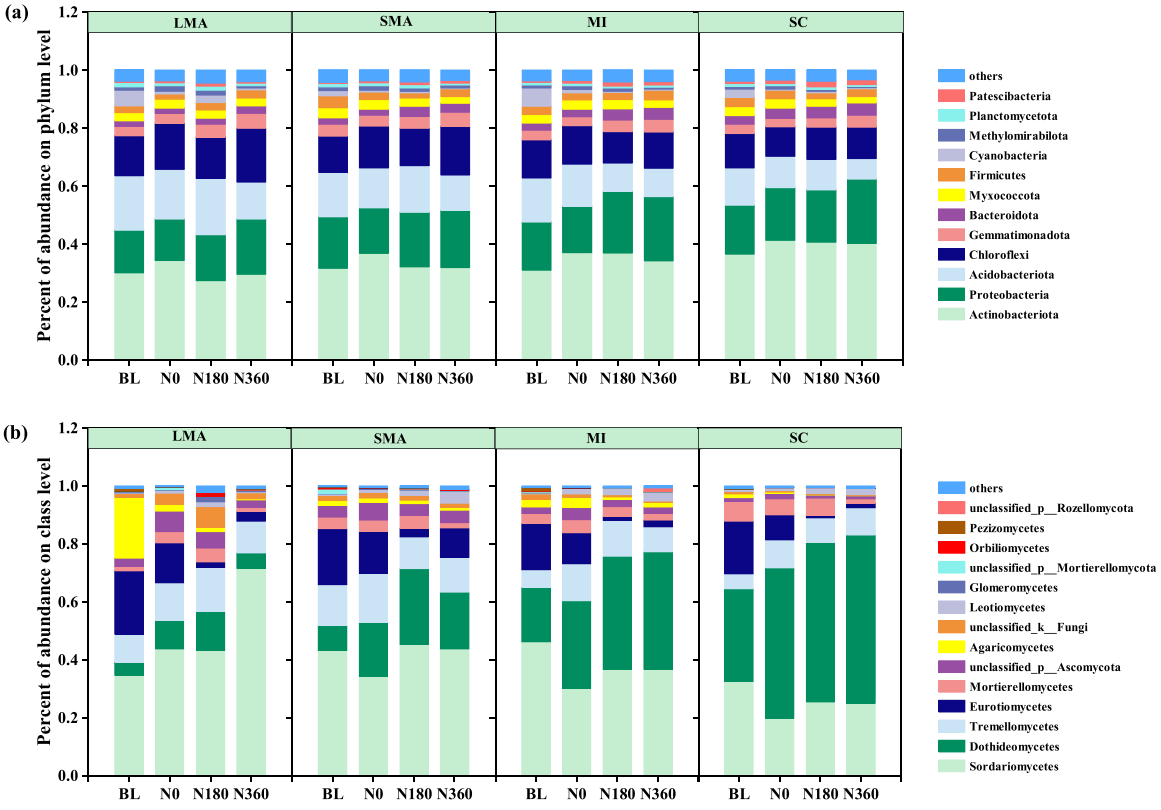

Fig. 3. Relative abundance on phylum level of bacterial communities (a) and class level of fungal communities (b) under N addition in aggregate fractions. LMA, large macroaggregate; SMA, small macroaggregate; MI, microaggregate; SC, silt-clay fractions. *Sordariomycetes*, *Dothideomycetes*, *Eurotiomycetes*, *unclassified_p_Ascomycota*, *Leotiomycetes*, *Orbiliomycetes*, and *Pezizomycetes* belong to *Ascomycota*, *Tremellomycetes* and *Agaricomycetes* belong to *Basidiomycota*, and *Mortierellomycetes* and *unclassified_p_Mortierellomycota* belong to *Mortierellomycota*.

($P < 0.001$). After N addition, the networks had more nodes and a higher average degree under N addition, indicating that N addition led to a more complex microbial network. Analogously, N addition enhanced connectivity and shortened the average path length, thereby tightening the networks. This is consistent with recent findings that N addition increases the complexity of the rhizosphere and non-rhizosphere networks (Wang et al., 2022). The main reasons for the more complex and tightening networks with N addition are that N fertilizer alters soil properties, microorganisms may increase interactions to adapt to environmental changes, and network complexity has a stronger impact on ecosystem function than soil microbial community diversity (Morrien et al., 2017). On one hand, N addition increases the availability of resources, and microorganisms increase resource transformation efficiency through enhanced cooperation (Zhao et al., 2019). On the other hand, high N input is detrimental to microbial growth, and microbes may enhance system stability through closer

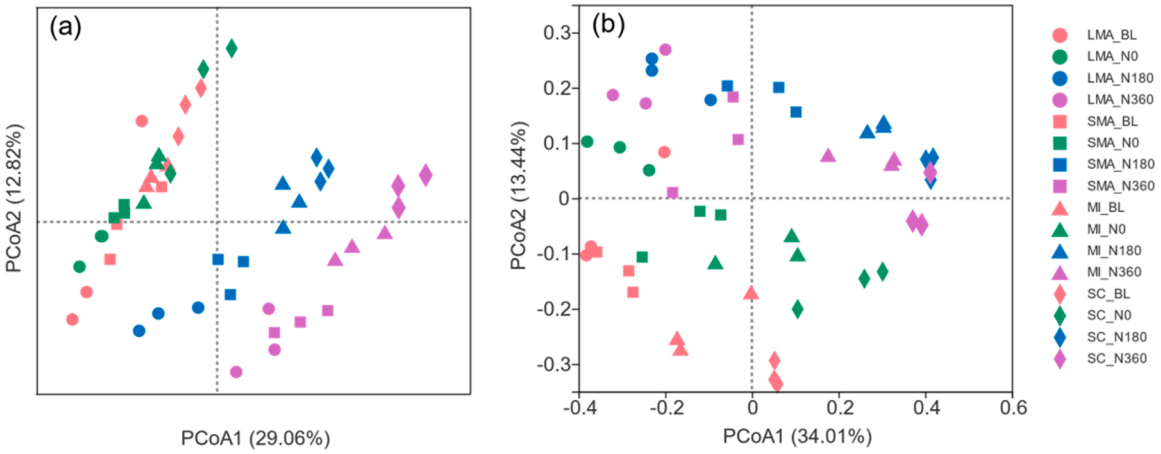

Fig. 4. Principal coordinate analysis based on the Bray-Curtis distances showing the effects of the N treatments and aggregate fractions on bacterial (a) and fungal (b) communities. Different colors represent different N treatments, and different symbols indicate different aggregate fractions. LMA, large macroaggregate; SMA, small macroaggregate; MI, microaggregate; SC, silt-clay fractions.

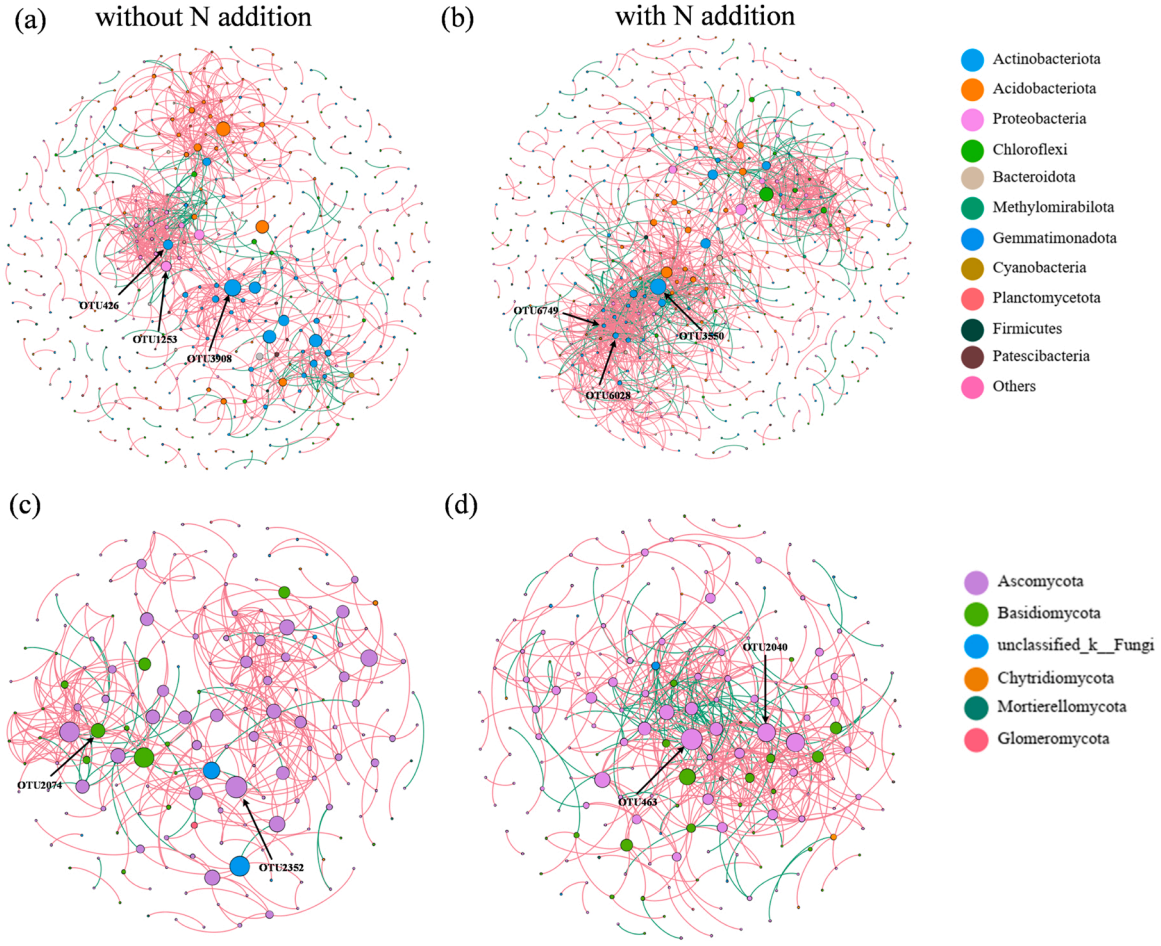

Fig. 5. Co-occurrence networks of bacterial (a, b) and fungal (c, d) communities of OTUs with and without N addition. The size of each node is proportional to the node betweenness, and the thickness of each connection between two nodes is proportional to the value of the Pearson correlation coefficients. A red edge indicates a positive interaction, while a green edge indicates a negative interaction. The OTUs shown in the figure represent keystone taxa.

association to resist unfavorable environmental conditions (Dong et al., 2022). Additionally, changes in the soil physical conditions can also affect network tightening. N addition affects the aggregate distribution proportion (Table 1), and heterogeneous habitats in aggregate size classes increase the co-occurrence pattern of microorganisms and promote network tightening (Liao et al., 2020).

Additionally, the nodes and degrees of the microaggregate networks were higher than those of the large macroaggregates. This is supported by previous findings, indicating that microbial networks are less connected in macroaggregates (Sun et al., 2022). Large macroaggregates accumulate labile C, while microaggregates accumulate recalcitrant C. Therefore, the recalcitrant C decomposition in microaggregates may

Table 2
Topological features of bacteria and fungi co-occurrence network.

Topological features	Bacteria		Fungi	
	without N	N	without N	N
Nodes	493	558	173	198
Edges	974	1425	409	535
R square of power-law	0.936	0.885	0.886	0.907
Average degree	3.951	5.108	4.728	5.404
Average clustering coefficient	0.179	0.188	0.254	0.265
Average path length	5.532	4.939	4.540	3.833
Density	0.008	0.009	0.027	0.027
Modularity	0.740	0.619	0.625	0.491
Positive/Negative	5.203	4.163	11.033	3.864

require microbial cooperation, resulting in complex networks (Fan et al., 2021a). Further, combined with mantel correlation analysis, network topological parameters were closely related to environmental factors ($P < 0.001$), suggesting that microaggregates had more favorable ecological niches, owing to greater availability of resources. Moreover, previous studies have shown that network complexity is positively correlated with its corresponding microbial diversity, i.e., more diverse and abundant microorganisms allow different taxa to complement each other with a greater likelihood of engaging in potential interactions, leading to more complex association networks (Chen et al., 2022; Han et al., 2022). It can also be explained that microaggregates have more complex networks due to a greater abundance of microorganisms (Chen et al., 2022). Silt-clay fractions also had a more complex network structure because more connected complex networks are more adaptable to the environment than less connected simple networks (Santolini and Barabasi, 2018). However, the bacterial and fungal co-occurrence patterns were based on the interactions between OTUs abundance and reflected potential interactions, and thus, require further functional validation.

4.3. Effects of N addition on C_{min} within aggregates

Carbon mineralization is the most important biochemical process in the soil, regulating the nutrient release and maintaining soil fertility (Xiao et al., 2022). C_{min} is influenced by factors such as the absolute amount of microbes and mineralizable organic carbon, and increasing

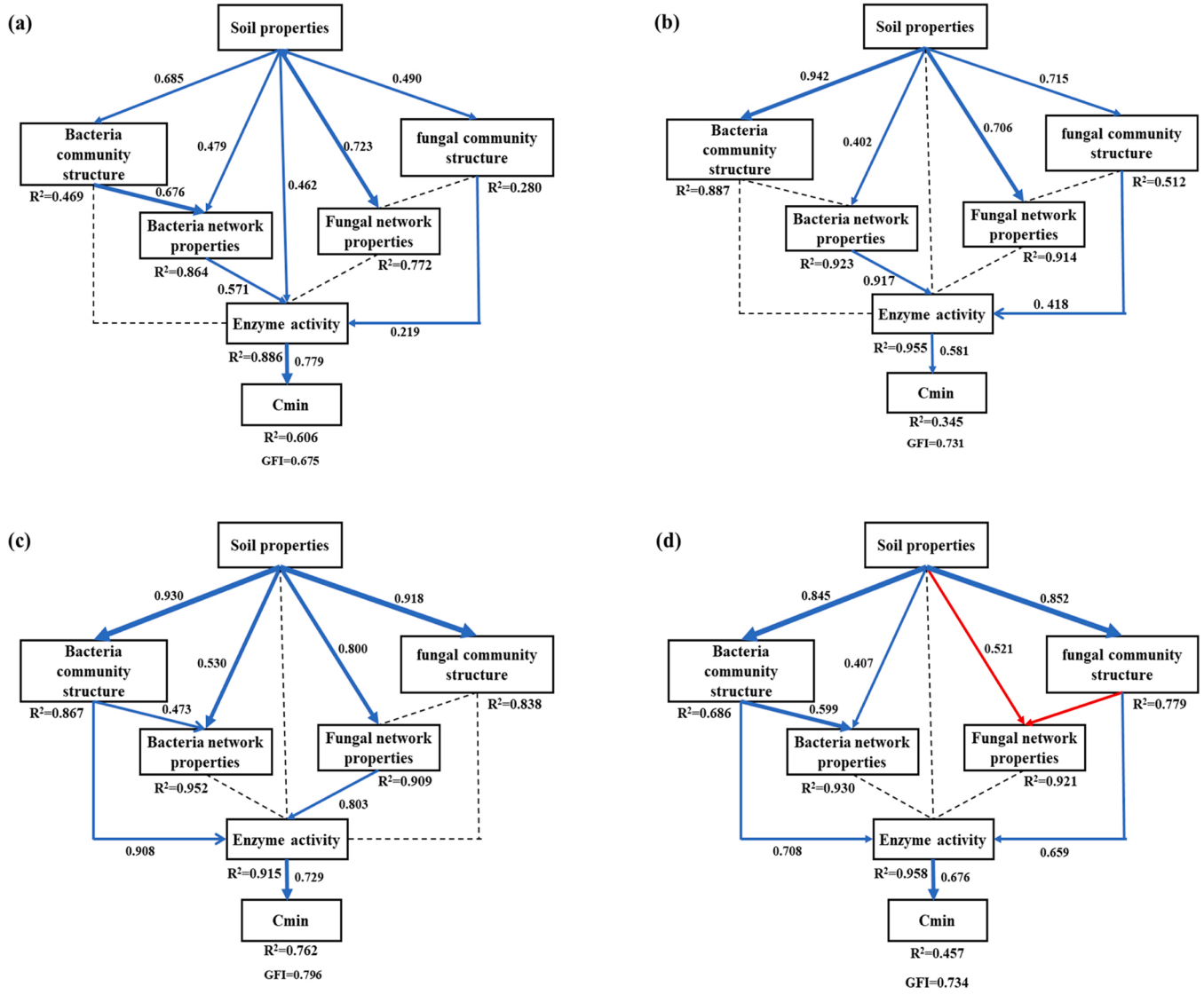

Fig. 6. Effects of soil properties, microbial community composition and microbial network topological properties on C mineralization in large macroaggregates (a), small macroaggregates (b), microaggregates (c), and silt-clay fractions (d) estimated using partial least squares path models (PLS-PM). The width of arrows indicates the strength of significant standardized path coefficients ($P < 0.05$). Blue lines indicate significant positive relationships. Red lines indicate significant negative relationships. The model was evaluated using goodness of fit (GFI).

evidence has shown that microbial communities and their interactions influence C dynamics (Morrien et al., 2017; Wang et al., 2021). In the present study, long-term N addition promoted C_{min} within aggregates. Additionally, N addition increased the SOC concentration across all aggregate fractions, and the cumulative C_{min} varied similarly to SOC concentration. The variation in cumulative C_{min} among aggregate sizes was also consistent with the SOC concentration, followed by the highest cumulative C_{min} observed for microaggregates and the lowest cumulative C_{min} for silt-clay fractions (Fig. 1). The variations in C_{min} for different aggregate sizes under N addition were caused by the heterogeneity of available resources (Wang et al., 2021). Correlation analysis indicated C_{min} to be significantly positively correlated with environmental factors, e.g., significantly positively correlated with SOC concentration ($P < 0.05$) and highly significantly positively correlated with DOC ($P < 0.01$; Table S9), and both of these results support the aforementioned conclusion. Many studies have shown that DOC as a labile carbon substrate for microorganisms, the conversion of which was closely related to the C_{min} (Dong et al., 2022). The amount and structure of SOC were unevenly distributed within the aggregate fractions, and different SOC fractions had different decomposition rates and turnover times (Lou et al., 2011). Generally, macroaggregates contain more fresh labile organic carbon and exhibit faster turnover. In contrast, SOC is more stable and has a longer turnover time in smaller aggregate fractions (Six et al., 2002). Thus, the spatial heterogeneity of nutrients available in different aggregate sizes strongly selects for microbial lifestyle and influences the distribution of microbial communities, which in turn affects the C_{min} processes. Although N addition exhibited a facilitative effect on C_{min} across aggregates, the driving mechanism varied depending on the aggregate sizes.

PLS-PM analysis revealed that soil properties influenced the production of extracellular enzymes, and consequently, had an impact on C_{min}, by affecting the microbial community and their interactions (Fig. 6). Large macroaggregates contained more fresh SOM, which led to the enrichment of specific microbial taxa. For example, *Chloroflexi* species are likely to prefer labile C (Hug et al., 2013). Compared with N addition, fungi were more influenced by aggregate fractions based on PERMANOVA (Table S2). Large macroaggregates have higher spatial heterogeneity and may benefit from fungal colonization and fungal hyphae entangling with soil particles to form macroaggregates (Ven et al., 2020), whereby *Basidiomycota* and *Glomeromycota* are more abundant in large macroaggregates. The increase in *Ascomycete* due to N addition promoted C_{min} in the macroaggregates (Table S8). Therefore, fungal community composition also affected C_{min} in the macroaggregates. However, interactions between faster-growing bacteria played a more dominant role than those between fungi. The mode of small aggregates was similar to that of large macroaggregates. Whereas microaggregates have more stable C, decomposing recalcitrant C and overcoming adverse soil conditions requires more species and stronger cooperative interactions between species, i.e. more complex and tight microbial networks (Morrien et al., 2017). The bacterial community composition and fungal networks collectively dominated the C_{min} response to N addition. Fungi are more conducive to decomposing recalcitrant C, and fungal network interactions are enhanced and more complex in microaggregates than in macroaggregates. Fungi in microaggregates may preferentially perform similar or complementary functions, resulting in synergistic interactions to utilize the substrates (Miao et al., 2022). Meanwhile, the relative abundance of *Actinomycetes* and *Proteobacteria* were greatest in microaggregates, corresponding to the more abundant available resources in the microaggregates, leading to a dominant role of the bacterial community composition for C_{min} in response to N addition. The silt-clay fractions have a lower C_{min} efficiency, owing to their low porosity and oxygen content (Fan et al., 2021a). Microbial interactions may be less important than community composition, which would result in microbial interactions that are not the dominant factors affecting C_{min}. Previous studies have shown that the SOC of silt-clay fractions is highly sensitive to fertilization (Jiang et al., 2017); we also noted that N addition increased oxidizable organic carbon in silt-clay fractions (unpublished data), which led to a greater effect of bacterial communities on the increase in C_{min} than fungi.

5. Conclusion

Long-term N addition increased C_{min} within the aggregate fractions and changed the microbial community composition and interaction patterns. Compared to with bacteria, the effect of aggregate fractions on fungi was greater than that of N addition. The resource spatial heterogeneity of different aggregate sizes strongly selected microbial lifestyles and influenced the distribution and coexistence patterns of microbial communities, leading to differences in the C_{min} with N addition. The bacterial co-occurrence pattern dominates C_{min} and is in concert with the fungal community composition to promote C_{min} in macroaggregates. The microaggregate bacterial community composition and fungal networks jointly dominated C_{min} in response to N addition. The microbial community composition in the silt-clay fractions dominated C_{min}. Our results elucidated the effects of N addition on C_{min} at the aggregate scale and highlighted the importance of co-occurrence networks as a key component of the functional linkage between microbial species composition and ecosystems. In conclusion, this study provided novel insights into the importance of microbes in regulating of C turnover at the microscale.

Declaration of Competing Interest

All the authors declare no conflict of interest.

Data Availability

Data will be made available on request.

Acknowledgements

This study was sponsored by the Strategic Priority Research Program of the Chinese Academy of Sciences (grant number XDA23070201), the National Natural Science Foundation of China (grant numbers 42077452).

Appendix A. Supporting information

Supplementary data associated with this article can be found in the online version at doi:10.1016/j.agee.2022.108249.

References

Allison, S.D., Gartner, T.B., Mack, M.C., McGuire, K., Treseder, K., 2010. Nitrogen alters carbon dynamics during early succession in boreal forest. Soil Biol. Biochem. 42, 1157–1164.
Bach, E.M., Williams, R.J., Hargreaves, S.K., Yang, F., Hofmockel, K.S., 2018. Greatest soil microbial diversity found in micro-habitats. Soil Biol. Biochem. 118, 217–226.
Badr, E., Achterberg, E.P., Tappin, A.D., Hill, S.J., Braungardt, C.B., 2003. Determination of dissolved organic nitrogen in natural waters using high-temperature catalytic oxidation. TrAC Trends Anal. Chem. 22, 819–827.
Banerjee, S., Kirkby, C.A., Schmutter, D., Bissett, A., Kirkegaard, J.A., Richardson, A.E., 2016. Network analysis reveals functional redundancy and keystone taxa amongst bacterial and fungal communities during organic matter decomposition in an arable soil. Soil Biol. Biochem. 97, 188–198.
Barberán, A., Bates, S.T., Casamayor, E.O., Fierer, N., 2012. Using network analysis to explore co-occurrence patterns in soil microbial communities. ISME J. 6, 343–351.
Bell, C.W., Fricks, B.E., Rocca, J.D., Steinweg, J.M., McMahon, S.K., Wallenstein, M.D., 2013. High-throughput fluorometric measurement of potential soil extracellular enzyme activities. J. Vis. Exp. 16.
Berry, D., Widder, S., 2014. Deciphering microbial interactions and detecting keystone species with co-occurrence networks. Front. Microbiol. 5, 219.
Bimueller, C., Kreyling, O., Koelbl, A., von Luetzow, M., Koegel-Knabner, I., 2016. Carbon and nitrogen mineralization in hierarchically structured aggregates of different size. Soil Tillage Res. 160, 23–33.
Bremner, J., Mulvaney, C., 1996. Nitrogen-total. Methods of Soil Analysis Chemical Methods Part 72, 532–535.

Chen, W., Wang, J., Chen, X., Meng, Z., Xu, R., Duoji, D., Zhang, J., He, J., Wang, Z., Chen, J., Liu, K., Hu, T., Zhang, Y., 2022. Soil microbial network complexity predicts ecosystem function along elevation gradients on the Tibetan Plateau. Soil Biol. Biochem. 172, 108766.
Deng, Y., Jiang, Y.-H., Yang, Y., He, Z., Luo, F., Zhou, J., 2012. Molecular ecological network analyses. BMC Bioinform. 13 (1), 113.
Dong, K., Yu, Z., Kerfahi, D., Lee, S.-S., Li, N., Yang, T., Adams, J.M., 2022. Soil microbial co-occurrence networks become less connected with soil development in a high Arctic glacier foreland succession. Sci. Total Environ. 813, 152565.
Dorodnikov, M., Blagodatskaya, E., Blagodatsky, S., Fangmeier, A., Kuzyakov, Y., 2009. Stimulation of r- vs. K-selected microorganisms by elevated atmospheric CO_2 depends on soil aggregate size. FEMS Microbiol. Ecol. 69, 43–52.
Fan, J., Jin, H., Zhang, C., Zheng, J., Zhang, J., Han, G., 2021a. Grazing intensity induced alternations of soil microbial community composition in aggregates drive soil organic carbon turnover in a desert steppe. Agric. Ecosyst. Environ. 313, 107387.
Fan, M., Li, J., Yan, W., Shi, H., Zhouping, S., 2021b. Shifts in the structure and function of wheat root-associated bacterial communities in response to long-term nitrogen addition in an agricultural ecosystem. Appl. Soil Ecol. 159, 103852.
Fierer, N., Lauber, C.L., Ramirez, K.S., Zaneveld, J., Bradford, M.A., Knight, R., 2012. Comparative metagenomic, phylogenetic and physiological analyses of soil microbial communities across nitrogen gradients. ISME J. 6, 1007–1017.
Fox, A., Ikoyi, I., Torres-Sallan, G., Lanigan, G., Schmalenberger, A., Wakelin, S., Creamer, R., 2018. The influence of aggregate size fraction and horizon position on microbial community composition. Appl. Soil Ecol. 127, 19–29.
Han, L., Xu, M., Kong, X., Liu, X., Wang, Q., Chen, G., Xu, K., Nie, J., 2022. Deciphering the diversity, composition, function, and network complexity of the soil microbial community after repeated exposure to a fungicide boscalid. Environ. Pollut. 312, 120060.
He, J., Jiao, S., Tan, X., Wei, H., Ma, X., Nie, Y., Liu, J., Lu, X., Mo, J., Shen, W., 2021. Adaptation of soil fungal community structure and assembly to long- versus short-term nitrogen addition in a tropical forest. Front. Microbiol. 12, 689674-689674.
Hug, L.A., Castelle, C.J., Wrighton, K.C., Thomas, B.C., Sharon, I., Frischkorn, K.R., Williams, K.H., Tringe, S.G., Banfield, J.F., 2013. Community genomic analyses constrain the distribution of metabolic traits across the Chloroflexi phylum and indicate roles in sediment carbon cycling. Microbiome 1 (1), 22.
Jia, J., Cao, Z., Liu, C., Zhang, Z., Lin, L., Wang, Y., Haghipour, N., Wacker, L., Bao, H., Dittmar, T., Simpson, M.J., Yang, H., Crowther, T.W., Eglinton, T.I., He, J.-S., Feng, X., 2019. Climate warming alters subsoil but not topsoil carbon dynamics in alpine grassland. Glob. Change Biol. 25, 4383–4393.
Jia, X., Zhong, Y., Liu, J., Zhu, G., Shangguan, Z., Yan, W., 2020. Effects of nitrogen enrichment on soil microbial characteristics: From biomass to enzyme activities. Geoderma 366, 114256.
Jiang, M., Wang, X., Liusui, Y., Han, C., Zhao, C., Liu, H., 2017. Variation of soil aggregation and intra-aggregate carbon by long-term fertilization with aggregate formation in a grey desert soil. Catena 149, 437–445.
Li, S., Wang, S., Fan, M., Wu, Y., Shangguan, Z., 2020. Interactions between biochar and nitrogen impact soil carbon mineralization and the microbial community. Soil Tillage Res. 196, 104437.
Liao, H., Zhang, Y., Wang, K., Hao, X., Chen, W., Huang, Q., 2020. Complexity of bacterial and fungal network increases with soil aggregate size in an agricultural Inceptisol. Appl. Soil Ecol. 154, 103640.
Ling, N., Chen, D., Guo, H., Wei, J., Bai, Y., Shen, Q., Hu, S., 2017. Differential responses of soil bacterial communities to long-term N and P inputs in a semi-arid steppe. Geoderma 292, 25–33.
Lombard, L., van der Merwe, N.A., Groenewald, J.Z., Crous, P.W., 2015. Generic concepts in Nectriaceae. Stud. Mycol. 80, 189–245.
Lou, Y.L., Wang, J.K., Liang, W.J., 2011. Impacts of 22-year organic and inorganic N managements on soil organic C fractions in a maize field, northeast China. Catena 87, 386–390.
Miao, Y., Lin, Y., Chen, Z., Zheng, H., Niu, Y., Kuzyakov, Y., Liu, D., Ding, W., 2022. Fungal key players of cellulose utilization: microbial networks in aggregates of long-term fertilized soils disentangled using 13C-DNA-stable isotope probing. Sci. Total Environ. 832, 155051-155051.
Moorhead, D.L., Rinkes, Z.L., Sinsabaugh, R.L., Weintraub, M.N., 2013. Dynamic relationships between microbial biomass, respiration, inorganic nutrients and enzyme activities: informing enzyme-based decomposition models. Front. Microbiol. 4, 223.
Morrien, E., Hannula, S.E., Snoek, L.B., Helmsing, N.R., Zweers, H., de Hollander, M., Soto, R.L., Bouffaud, M.-L., Buee, M., Dimmers, W., Duyts, H., Geisen, S., Girlanda, M., Griffiths, R.I., Jorgensen, H.-B., Jensen, J., Plassart, P., Redecker, D., Schmelz, R.M., Schmidt, O., Thomson, B.C., Tisserant, E., Uroz, S., Winding, A., Bailey, M.J., Bonkowski, M., Faber, J.H., Martin, F., Lemanceau, P., de Boer, W., van Veen, J.A., van der Putten, W.H., 2017. Soil networks become more connected and take up more carbon as nature restoration progresses. Nat. Commun. 8, 14349.
Murphy, J., Riley, J.P., 1962. A modified single solution method for the determination of phosphate in natural waters. Anal. Chim. Acta 27, 31–36.
Nelson, D.W., Sommers, L.E., 1982. Total carbon, organic carbon and organic matter. In: Page, A.L., Miller, R.H., Keeney, D.R. (Eds.), methods of soil analysis, Part 2. American Society of Agronomy, pp. 539–579.
Olsen, S.R., Sommers, L.E., 1982. Phosphorous. In: Page, A.L., Miller, R.H., Keeney, D.R. (Eds.), Methods of Soil Analysis, Part 2, Chemical and Microbial Properties. Agronomy Society of America, Madison, pp. 403–430.
Polme, S., Abarenkov, K., Henrik Nilsson, R., Lindahl, B.D., Clemmensen, K.E., Kauserud, H., Nguyen, N., Kjoller, R., Bates, S.T., Baldrian, P., Froslev, T.G., Adojaan, K., Vizzini, A., Suija, A., Pfister, D., Baral, H.-O., Jarv, H., Madrid, H., Norden, J., Liu, J.-K., Pawlowska, J., Poldmaa, K., Partel, K., Runnel, K., Hansen, K., Larsson, K.-H., Hyde, K.D., Sandoval-Denis, M., Smith, M.E., Toome-Heller, M., Wijayawardene, N.N., Menolli, N., Reynolds, Jr, Drenkhan, N.K., Maharachchikumbura, R., Gibertoni, S.S.N., Laessoe, T.B., Davis, T., Tokarev, W., Corrales, Y., Soares, A., Agan, A.M., Machado, A., Arguelles-Moyao, A.R., Detheridge, A., de Meiras-Ottoni, A., Verbeken, A., Dutta, A., Cui, A.K., Pradeep, B.-K., Marin, C.K., Stanton, C., Gohar, D., Wanasinghe, D., Otsing, D.N., Aslani, E., Griffith, F., Lumbsch, G.W., Grossart, T.H., Masigol, H.-P., Timling, H., Hiiesalu, I., Oja, I., Kupagme, J., Geml, J.Y., Alvarez-Manjarrez, J., Ilves, J., Loit, K., Adamson, K., Nara, K., Kungas, K., Rojas-Jimenez, K., Bitenieks, K., Irinyi, K., Nagy, L., Soonvald, L.L., Zhou, L., Wagner, L.-W., Aime, L., opik, M, M.C., Mujica, M. I., Metsoja, M., Ryberg, M., Vasar, M., Murata, M., Nelsen, M.P., Cleary, M., Samarakoon, M.C., Doilom, M., Bahram, M., Hagh-Doust, N., Dulya, O., Johnston, P., Kohout, P., Chen, Q., Tian, Q., Nandi, R., Amiri, R., Perera, R.H., dos Santos Chikowski, R., Mendes-Alvarenga, R.L., Garibay-Orijel, R., Gielen, R., Phookamsak, R., Jayawardena, R.S., Rahimlou, S., Karunarathna, S.C., Tibpromma, S., Brown, S.P., Sepp, S.-K., Mundra, S., Luo, Z.-H., Bose, T., Vahter, T., Netherway, T., Yang, T., May, T., Varga, T., Li, W., Coimbra, V.R.M., de Oliveira, V. R.T., de Lima, V.X., Mikryukov, V.S., Lu, Y., Matsuda, Y., Miyamoto, Y., Koljalg, U., Tedersoo, L., 2020. FungalTraits: a user-friendly traits database of fungi and fungus-like stramenopiles. Fungal Divers. 105, 1–16.
Rabbi, S.M.F., Wilson, B.R., Lockwood, P.V., Daniel, H., Young, I.M., 2014. Soil organic carbon mineralization rates in aggregates under contrasting land uses. Geoderma 216, 10–18.
Rabbi, S.M.F., Daniel, H., Lockwood, P.V., Macdonald, C., Pereg, L., Tighe, M., Wilson, B. R., Young, I.M., 2016. Physical soil architectural traits are functionally linked to carbon decomposition and bacterial diversity. Sci. Rep. 6, 33012.
Ren, H., Huang, B., Fernandez-Garcia, V., Miesel, J., Yan, L., Lv, C., 2020. Biochar and rhizobacteria amendments improve several soil properties and bacterial diversity. Microorganisms 8, 502.
Ruamps, L.S., Nunan, N., Chenu, C., 2011. Microbial biogeography at the soil pore scale. Soil Biol. Biochem. 43, 280–286.
Santolini, M., Barabasi, A.-L., 2018. Predicting perturbation patterns from the topology of biological networks. Proc. Natl. Acad. Sci. USA 115, E6375–E6383.
Six, J., Elliott, E.T., Paustian, K., 2000. Soil macroaggregate turnover and microaggregate formation: a mechanism for C sequestration under no-tillage agriculture. Soil Biol. Biochem. 32, 2099–2103.
Six, J., Conant, R.T., Paul, E.A., Paustian, K., 2002. Stabilization mechanisms of soil organic matter: Implications for C-saturation of soils. Plant Soil 241, 155–176.
Six, J., Bossuyt, H., Degryze, S., Denef, K., 2004. A history of research on the link between (micro)aggregates, soil biota, and soil organic matter dynamics. Soil Tillage Res. 79, 7–31.
Su, X., Su, X., Zhou, G., Du, Z., Yang, S., Ni, M., Qin, H., Huang, Z., Zhou, X., Deng, J., 2020. Drought accelerated recalcitrant carbon loss by changing soil aggregation and microbial communities in a subtropical forest. Soil Biol. Biochem. 148, 107898.
Sun, D., Lin, Q., Angst, G., Huang, L., Aniko, C., Emsens, W.-J., van Diggelen, R., Vicena, J., Cajthaml, T., Frouz, J., 2022. Microbial communities in soil macro-aggregates with less connected networks respire less across successional and geographic gradients. Eur. J. Soil Biol. 108, 103378.
Tian, J., Pausch, J., Yu, G., Blagodatskaya, E., Kuzyakov, Y., 2016. Aggregate size and glucose level affect priming sources: A three-source-partitioning study. Soil Biol. Biochem. 97, 199–210.
Ven, A., Verbruggen, E., Verlinden, M.S., Olsson, P.A., Wallander, H., Vicca, S., 2020. Mesh bags underestimated arbuscular mycorrhizal abundance but captured fertilization effects in a mesocosm experiment. Plant Soil 446, 563–575.
Wang, J., Liao, L., Ye, Z., Liu, H., Zhang, C., Zhang, L., Liu, G., Wang, G., 2022. Different bacterial co-occurrence patterns and community assembly between rhizosphere and bulk soils under N addition in the plant-soil system. Plant Soil 471, 697–713.
Wang, R., Dorodnikov, M., Yang, S., Zhang, Y., Filley, T.R., Turco, R.F., Zhang, Y., Xu, Z., Li, H., Jiang, Y., 2015. Responses of enzymatic activities within soil aggregates to 9-year nitrogen and water addition in a semi-arid grassland. Soil Biol. Biochem. 81, 159–167.
Wang, W., Chen, D., Sun, X., Zhang, Q., Koide, R.T., Insam, H., Zhang, S., 2019. Impacts of mixed litter on the structure and functional pathway of microbial community in litter decomposition. Appl. Soil Ecol. 144, 72–82.
Wang, X., Bian, Q., Jiang, Y., Zhu, L., Chen, Y., Liang, Y., Sun, B., 2021. Organic amendments drive shifts in microbial community structure and keystone taxa which increase C mineralization across aggregate size classes. Soil Biol. Biochem. 153, 108062.
Xiao, D., He, X., Wang, G., Xu, X., Hu, Y., Chen, X., Zhang, W., Su, Y.A., Wang, K., Soromotin, A.V., Alharbi, H.A., Kuzyakov, Y., 2022. Network analysis reveals bacterial and fungal keystone taxa involved in straw and soil organic matter mineralization. Appl. Soil Ecol. 173, 104395.
Zeng, J., Liu, X., Song, L., Lin, X., Zhang, H., Shen, C., Chu, H., 2016. Nitrogen fertilization directly affects soil bacterial diversity and indirectly affects bacterial community composition. Soil Biol. Biochem. 92, 41–49.
Zhang, H., Wang, S., Zhang, J., Tian, C., Luo, S., 2021a. Biochar application enhances microbial interactions in mega-aggregates of farmland black soil. Soil Tillage Res. 213, 105145.
Zhang, Q., Cheng, L., Feng, J., Mei, K., Zeng, Q., Zhu, B., Chen, Y., 2021b. Nitrogen addition stimulates priming effect in a subtropical forest soil. Soil Biol. Biochem. 160, 108339.
Zhao, S., Fan, F., Qiu, S., Xu, X., He, P., Ciampitti, I.A., 2021. Dynamic of fungal community composition during maize residue decomposition process in north-central China. Appl. Soil Ecol. 167, 104057.
Zhao, Z.-B., He, J.-Z., Geisen, S., Han, L.-L., Wang, J.-T., Shen, J.-P., Wei, W.-X., Fang, Y.-T., Li, P.-P., Zhang, L.-M., 2019. Protist communities are more sensitive to nitrogen

fertilization than other microorganisms in diverse agricultural soils. Microbiome 7, 33.
Zheng, H., Wang, X., Luo, X., Wang, Z., Xing, B., 2018. Biochar-induced negative carbon mineralization priming effects in a coastal wetland soil: roles of soil aggregation and microbial modulation. Sci. Total Environ. 610, 951–960.
Zhong, Y., Yan, W., Shangguan, Z., 2015. Soil carbon and nitrogen fractions in the soil profile and their response to long-term nitrogen fertilization in a wheat field. Catena 135, 38–46.